The New World Arenavirus Tacaribe induces caspase-dependent apoptosis in infected cells

Svenja Wolff[1,6], Allison Groseth[1,*], Bjoern Meyer[3,#], David Jackson[3], Thomas Strecker[1], Andreas Kaufmann[4], Stephan Becker[1,6]

[1] Institut für Virologie, Philipps-Universität Marburg,
Hans-Meerwein Str. 2, 35043 Marburg, Germany
[3] University of St. Andrews, Biomedical Sciences Research Complex,
North Haugh, St. Andrews, Fife, KY16 9ST Scotland
[4] Institut für Immunologie, Philipps-Universität Marburg,
Hans-Meerwein Str. 2, 35043 Marburg, Germany
[6] German Center for Infection Research (DZIF), partner site Giessen-Marburg-Langen,
Hans-Meerwein Str. 2, 35043 Marburg, Germany Marburg
* Present address: Friedrich-Loeffler-Institut,
Südufer 10, 17493 Greifswald - Insel Riems, Germany
[#] Present address: Department of Veterinary and Biomedical Sciences, University of Minnesota,
Falcon Heights, MN 55108, Twin Cities, USA

Corresponding author:
Prof. Dr. Stephan Becker
Institut für Virologie, Philipps-Universität Marburg
Hans-Meerwein Str. 2, 35043 Marburg, Germany
Phone: +49 6421 28 66253
Fax: +49 6421 28 68962
E-mail: becker@staff.uni-marburg.de

Running Title: Induction of apoptosis by Tacaribe virus

Word Counts:
Summary max 250 words: 226
Main text (introduction, results, discussion, methods) max 6500 words: 5344
Number of Figures: 6

Summary

The *Arenaviridae* is a diverse and growing family of viruses that already includes more than 25 distinct species. While some of these viruses have a significant impact on public health, others appear to be non-pathogenic. At present little is known about the host cell responses to infection with different arenaviruses, particularly those found in the New World, however, apoptosis is known to play an important role in controlling infection of many viruses. Here we show that infection with Tacaribe virus (TCRV), which is widely considered the prototype for non-pathogenic arenaviruses, leads to stronger induction of apoptosis than does infection with its human pathogenic relative Junín virus (JUNV). TCRV-induced apoptosis occurred in several cell types during late stages of infection and was shown to be caspase-dependent, involving the activation of caspases 3, 7, 8, and 9. Further, UV-inactivated TCRV did not induce apoptosis, indicating that the activation of this process is dependent on active viral replication/transcription. Interestingly, when apoptosis was inhibited, growth of TCRV was not enhanced, indicating that apoptosis does not have a direct negative effect on TCRV infection *in vitro*. Taken together, our data identify and characterize an important virus-host cell interaction of the prototypic, non-pathogenic arenavirus TCRV, which provides important insight into the growing field of arenavirus research aimed at better understanding the diversity in responses to different arenavirus infections and their functional consequences.

Introduction

The *Arenaviridae* is a diverse and growing family of viruses including more than 25 distinct species that are characterized by their bi-segmented, single-stranded RNA genome, which employs an ambisense coding strategy on both segments. The smaller S segment (~3.5 kb) contains genes encoding the nucleoprotein (NP) and the glycoprotein precursor (GPC), while the larger L segment (~7.5 kb) encodes the RNA-dependent RNA polymerase (L) and the RING finger motif-containing matrix protein (Z). The proteins assemble to produce enveloped particles that are spherical and highly pleomorphic, with a diameter of 50 to 300 nm. Despite their similar attributes with respect to virion architecture and genome arrangement, the members of arenaviruses can be further divided into the Old World and New World arenaviruses, reflecting differences in their genetic and antigenic relationships as well as their geographic distribution (Briese *et al.*, 2009; King, 2009).

Several New World arenaviruses, which are also known as Tacaribe serocomplex viruses, including Junín (JUNV), Machupo, Chapare, Guanarito, and Sabiá viruses, cause distinct hemorrhagic fever diseases that are collectively referred to as South American Hemorrhagic Fevers. However, a number of New World arenaviruses have also been identified that are non-pathogenic for humans. A prime example is the prototype of this group, Tacaribe virus (TCRV), which is closely related to both JUNV and Machupo virus, but for which only a single case of laboratory-acquired febrile disease has been reported since its detection in 1956 (Carballal *et al.*, 1987; Peters, 1996; Weissenbacher *et al.*, 1975). So far, the basis for the observed differences in virulence remains unclear, and indeed little is known about the host cell responses to infection with these viruses.

Due to their close phylogenetic relationship, despite strong phenotypic difference, virus pairs like JUNV and TCRV provide an excellent opportunity to identify arenavirus pathogenicity factors. Using this approach, we have previously identified differences in the induction of cytokine responses to infection with TCRV or JUNV in macrophages, as well as differences in their influence on host cell apoptosis (Groseth *et al.*, 2010a; Wolff *et al.*, 2013a). Other known differences that also might play a role for the virulence include receptor usage (Abraham *et al.*, 2009), as well as the ability to engage in interferon (IFN) antagonism (Xing *et al.*, 2015). Previous studies have shown that TCRV lacks a novel NP-mediated anti-apoptotic function that was described for JUNV (Wolff *et al.*, 2013a), and together with the observation that TCRV infection also induces severe cytopathic effects (CPE) during infection in cell culture (Groseth *et*

al., 2010a), this suggests that cell death might be due at least in part to apoptotic responses. However, the extent to which apoptosis is in fact being induced during infection, as well as the biological role and significance of any induction of apoptotic pathways during TCRV infection, remained unclear.

Apoptosis is the process of programmed cell death and plays an important role in the host response to virus infection (Thompson *et al.*, 2011). Apoptosis can be initiated via the extrinsic pathway, mediated by death receptors of the TNF-family on the cell surface (Ashkenazi & Dixit, 1998), as well as the intrinsic pathway, triggered by the release of cytochrome c from the inner mitochondrial membrane into the cytosol (Granville & Gottlieb, 2002). Virus-induced apoptosis can be mediated via the extrinsic as well as the intrinsic signalling pathways and is most often initiated by viral replication/transcription and the accumulation of viral RNA and proteins in the cytoplasm of the host cell, as demonstrated for infections with West Nile virus, Newcastle Disease virus, Oropouche virus and Enterovirus (Acrani *et al.*, 2009; Kleinschmidt *et al.*, 2007; Ravindra *et al.*, 2008; Shih *et al.*, 2008). Both signalling pathways converge to proteolytically activate a cascade of cysteine-dependent aspartate-specific proteases (caspases) that are present as inactive pro-caspases in all cells. Initiator caspases (caspases 2, 8, 9, and 10) become activated by cleavage in the early apoptotic phase and are responsible for the cleavage of effector caspases (caspases 3, 6, and 7), which in turn cleave target host proteins to induce further steps of the cell's degradation (Ho & Hawkins, 2005; Kumar, 2007; Nunez *et al.*, 1998; Timmer & Salvesen, 2007). Furthermore, apoptosis can be mediated by caspase-independent pathways (Borner & Monney, 1999; Cande *et al.*, 2002; Daugas *et al.*, 2000; Green & Kroemer, 1998). Prominent hallmarks of apoptotic signalling include caspase and PARP (poly (ADP-ribose) polymerase) cleavage, and these signals culminate in classical morphological changes such as cell shrinking and chromatin condensation (Fischer *et al.*, 2003; Ivana Scovassi & Diederich, 2004).

Viruses have developed different mechanisms to modulate apoptotic processes in infected cells in order to induce optimal conditions for viral replication (Hay & Kannourakis, 2002; Richard & Tulasne, 2012; Roulston *et al.*, 1999). On the one hand, inhibition of apoptosis serves to extend the cell life-span and viruses are considered to benefit from the resulting continued availability of the cellular machinery needed for efficient virus replication. In contrast, some viruses benefit from cellular apoptosis (Hay & Kannourakis, 2002; Richard & Tulasne, 2012; Roulston *et al.*, 1999; Teodoro & Branton, 1997). For instance, influenza virus, astroviruses and Aleutian mink

disease virus all require infection-induced apoptosis for efficient viral replication and release (Best *et al.*, 2003; Mendez *et al.*, 2004; Olsen *et al.*, 1996; Wurzer *et al.*, 2003).

In this study, we show that infection with non-pathogenic TCRV leads to a much stronger induction of apoptosis than does infection with its human pathogenic relative JUNV. TCRV-induced apoptosis occurred in a variety of mammalian cell types during the late stages of infection. Further, we could show that TCRV-induced apoptosis is caspase-dependent and triggered by active viral replication/transcription, as seems to be linked to expression of the Z protein. Interestingly, TCRV replication was not diminished by enhanced caspase activity, suggesting that TCRV growth is not directly hindered by the induction of apoptosis in infected cells. Based on the close phylogenetic relationship between TCRV and other pathogenic members of the New World arenaviruses, a better understanding of host responses to TCRV infection is an important step in identifying factors associated with arenavirus virulence, and may ultimately help us to better predict the risk posed by newly emerging arenavirus species in future.

Results

Several lines of evidence had suggested that TCRV might be impaired in its ability to suppress apoptosis induction compared to JUNV (Groseth *et al.*, 2010a; Wolff *et al.*, 2013a), leading us to investigate whether TCRV infection indeed induces appreciable levels of apoptosis in infected cells, and if so, by what mechanisms. VeroE6 cells, which represent a highly permissive system for arenavirus infection and are defective in IFN secretion, were inoculated with TCRV at an MOI of 1 pfu/cell. Infection with Sendai virus (SeV, 20 HA/ml), which is known to be a potent inducer of apoptosis, served as a positive control (Gadaleta *et al.*, 2002). The formation of CPE in infected cells, as well as known hallmarks of apoptosis, including caspase 3 cleavage and chromatin condensation, were monitored. SeV infection resulted in caspase 3 cleavage which was already detectable at day 1 post-infection (p.i.), while TCRV infected cells showed caspase 3 cleavage starting at 2 days p.i. (Fig. 1a). These results were also consistent with the phenotype of the infected cells, which showed pronounced CPE formation and prominent chromatin condensation (Fig. 1b) 72 h after TCRV infection. To confirm these results, a Caspase-Glo 3/7 Assay was performed, showing that activity of the effector caspases 3 and 7 in VeroE6 cells was clearly enhanced on day 2 after TCRV infection (Fig. 1c). Chemical induction of apoptosis using camptothecin (CPT) served as positive control. Taken together, these data clearly indicate that TCRV infection of VeroE6 cells indeed induces apoptosis and that this induction occurs at later times p.i..

As apoptotic signalling was only induced by TCRV later in the infection, we presumed that, rather than virus binding, which is an extremely early event, active virus replication and/or accumulation of the products of virus infection might be necessary for apoptosis induction. To test this hypothesis, VeroE6 cells were infected either with viable TCRV at an MOI 1 or with the same quantity of UV-inactivated TCRV and analysed for the induction of apoptosis. While CPE formation was clearly detectable in TCRV infected VeroE6 cells, infection with UV-inactivated TCRV did not show any CPE compared to mock (Fig. 2a, middle panels). Microscopic analysis of DAPI stained cells also showed that apoptotic nuclei, while clearly observed for TCRV infected cells, were absent in the case of UV-inactivated virus (Fig. 2a, lower panel), confirming that apoptosis was not induced in these samples. For further characterization and quantification, Western blot analysis and a Caspase-Glo 3/7 Assay were performed. VeroE6 cells were infected with TCRV at an MOI of 1, as well as with the same quantity of UV-inactivated virus and analysed at the indicated time points. Infection of the cells with JUNV, which is known to show neither strong CPE formation nor chromatin condensation up to day 6 p.i. (MOI 1 and 3) (Wolff

et al., 2013a), served as additional control. In contrast to infection with JUNV, evidence of apoptotic signalling was clearly detectable in TCRV infected VeroE6 cells, as cleavage of caspase 3 and PARP, another marker of apoptosis, were observed (Fig. 2b). However, even six days after infection with UV-inactivated TCRV neither caspase 3 nor PARP cleavage were detectable (Fig. 2b). In addition, UV-inactivated TCRV did not significantly enhance caspase 3/7 activity (Fig. 2c). Interestingly, JUNV infected cells showed slight caspase 3/7 activity, too, but apoptotic signalling was much weaker than in TCRV infected cells under these conditions (Fig. 2c). Thus, these data clearly indicate that TCRV-induced apoptosis depends predominantly on active virus replication/transcription.

To investigate if TCRV-induced apoptosis is the result of the accumulation of viral proteins following virus replication in the infected cell, individual viral proteins were over-expressed and CPE formation as well as chromatin condensation was examined. Microscopic analysis at 48 h post-transfection (p.t.) revealed no CPE formation in samples expressing NP and only slight CPE formation in GPC-expressing VeroE6 cells (Fig. 2d, arrows). However, expression of TCRV Z induced a prominent CPE in conjunction with the accumulation of apoptotic nuclei, as well as caspase 3 cleavage, suggesting that the accumulation of Z during infection is a major factor contributing to the induction of apoptosis in TCRV infected VeroE6 cells (Figs. 2d, 2e).

We next sought to determine the caspase pathways activated in TCRV infected cells. Western blot analysis of TCRV infected cell lysates (MOI 1) showed that at day 3 p.i. cleavage of both initiator caspases 8 and 9 was detectable, with cleavage of caspase 9 being much more prominent (Fig. 3a). Infection with SeV (20 HA/ml), which is known to induce cleavage of both caspases 8 and 9 during infection, served as a positive control, with cleavage of both proteins being clearly detectable (Bitzer *et al.*, 2002; Bitzer *et al.*, 1999). As expected, infection with UV-inactivated TCRV did not induce cleavage of either caspase 8 or 9. Additional analysis of TCRV infected VeroE6 cells using Caspase-Glo Assays showed a clear and prominent activation of caspase 9 (Fig. 3b). However, while caspase 9 activity in TCRV infected cells was increased about 3-fold, in comparison to cells treated with UV-inactivated TCRV, caspase 8 activation remained low (<1.3-fold increase). Taken together, these data indicate that TCRV infection induces the activation of the effector caspases 3 and 7, via signalling pathways involving the initiator caspase 9, and to a much lesser extent caspase 8. This predominant activation of caspase 9 indicates that the induction of apoptosis by TCRV infection is occurring primarily via the intrinsic activation pathway.

To investigate whether TCRV-induced apoptosis is specific to VeroE6 cells, HuH7 cells and primary human macrophages, which are important primary target cells for arenaviruses, were additionally analysed. Cells were infected with TCRV (MOI 3) and at 72 h p.i. monitored for CPE formation, as well as for the expression of NP, to demonstrate the cells' susceptibility to TCRV infection (Fig. 4a). A Caspase-Glo 3/7 Assay showed in TCRV infected HuH7 cells, VeroE6 cells and primary human macrophages clear evidence of caspase activation (Fig. 4b). In comparison to VeroE6 cells, which showed an enhancement of caspase activity of around 2.5-fold, caspase activation in HuH7 cells was lower (1.5-fold increase) which corresponded to a lesser susceptibility of HuH7 cells to the chemical induction of apoptosis using CPT. The caspase activity in TCRV infected primary human macrophages on the other hand was notably higher than in VeroE6 cells (6-fold induction, Fig. 4b). Taken together, these data indicate that TCRV infection induces apoptotic signalling in a variety of mammalian cell types, including macrophages, and the degree of caspase activation seems to be cell type-dependent.

Interestingly, our previous findings showed that JUNV NP, but not TCRV NP, serves as a decoy substrate to diminish apoptosis during infection (Wolff *et al.*, 2013a), furthermore TCRV and JUNV infected VeroE6 cells differed in the induction of apoptosis and its associated signalling cascades (Fig. 2). While no apoptotic signalling was observed in JUNV infected cells by Western blot (Fig. 2b, caspase 3 and PARP cleavage), which is consistent with the lack of evidence for morphological changes, i.e. nuclear condensation and cell death, during JUNV infection (Wolff *et al.*, 2013a), the more sensitive Caspase-Glo Assay reveals that JUNV-induced caspase activation does take place, but at a very low level (Fig. 2c). Based on the findings that TCRV and JUNV, which differ in pathogenicity, also show obvious differences in apoptosis induction in VeroE6 cells, it was of strong interest to analyse this feature in primary human macrophages. Therefore, macrophages from two different donors were isolated and infected with TCRV and JUNV at an MOI of 1, as well as with the same amount of UV-inactivated viruses. At 72 h p.i., cells were monitored for CPE formation, as well as the expression of NP, to demonstrate infection (Fig. 5a), and analysed for caspase activity (Fig. 5b). As expected, TCRV infection of macrophages induced activity of all three caspases tested. Interestingly, upon JUNV infection, macrophages also reacted with a small but significant increase in caspase activity, which was more prominent than in VeroE6 cells. However, while TCRV infected human macrophages showed a 4-fold enhancement of caspase 3/7 activity, the enhancement of caspase activity was only 1.6-fold in the case of JUNV infection (Fig. 5b). Similar results could be observed for caspase 8 and 9 activity, which also showed a much more prominent increase during TCRV infection (2.1-fold, 3.1-fold) than during JUNV infection (1.3-fold, 1.25-fold) (Fig. 5b). Confirming

the results with VeroE6 cells, caspase 9 activation is also more prominent than is activation of caspase 8 in TCRV infected macrophages (Fig. 5b). These results indicate that TCRV infection induced apoptotic signalling in primary human macrophages mainly via caspase 9 as in VeroE6 cells, and confirmed that JUNV infection is only a weak inducer of caspase activation.

While the regulation of apoptosis during infection often represents an important factor for host survival and clearance of viral infections, this is not always the case. Indeed there are a number of well characterized examples of virus systems that specifically exploit these pathways to complete the viral life cycle. It was therefore of interest whether the induction of apoptotic responses indeed had a direct effect on TCRV infection. To accomplish this, VeroE6 cells were infected with TCRV (MOI 0.1) and growth kinetics were analysed in the presence and absence of the caspase inhibitor Z-VAD-FMK. While the inhibition of apoptosis using Z-VAD-FMK indeed resulted in reduced CPE formation in TCRV infected cells (Fig. 6a), virus titres in the supernatants of infected cells, as determined via plaque assay, showed a slight reduction in viral growth of about 0.5 log (Fig. 6a, graph). Based on this observation, growth kinetics were also performed in the presence of the apoptosis inducer CPT (0.5 µM and 1 µM), in order to determine if enhanced activation of caspases would have a corresponding positive influence on TCRV growth. As a control, the cells were treated with DMSO or Z-VAD-FMK. Indeed, despite lower cell numbers due to apoptosis induction, the viral titres on day 1 p.i. showed that additional activation of caspases by CPT slightly enhanced virus growth, again by 0.5 log (Fig. 6b, graph). As treatment with CPT led to significant cell death after day 2 p.i. (Fig. 6b), growth kinetics were only performed up to day 3 p.i.. For comparison of TCRV titres between CPT- or Z-VAD-FMK-treated cells, one-way ANOVA tests were used for statistical analysis at single time points. Overall these data suggest that during infection TCRV growth is not impaired by the enhancement of caspase activity.

Discussion

Apoptosis is widely recognized as an important factor in the antiviral host response. However, some viruses can also actively exploit this process to facilitate their replication cycle. In order to better understand the role of apoptosis induction, and particularly caspase activation during arenavirus infection, the mechanism and biological relevance of apoptosis induction were examined during infection with TCRV, the prototype of non-pathogenic New World arenaviruses.

TCRV infected cells showed significant hallmarks of apoptosis, i.e. cleavage and activation of different caspases, followed by PARP cleavage, as well as chromatin condensation, and the formation of apoptotic bodies. The induction of apoptosis was not induced by virus binding to the host cells but detected late during TCRV infection, starting at 48 to 72 h p.i.. These time points correlate with high levels of progeny virus production and release from the host cells. Apoptosis-inducing viruses of the family Bunyaviridae like Oropouche virus, Crimean-Congo hemorrhagic fever virus or Hantavirus show comparable time courses for the induction of apoptosis (Acrani et al., 2009; Karlberg et al., 2010), and for these viruses it was shown that apoptosis of the host cell was not induced by binding or entry of the virus but by viral replication (Acrani et al., 2009; Li et al., 2004; Rodrigues et al., 2013). Similarly, experiments with UV-inactivated viruses such as West Nile virus, Newcastle Disease Virus, Oropouche virus and Enterovirus have also identified a dependence on viral replication as the major apoptosis-inducing factor (Acrani et al., 2009; Kleinschmidt et al., 2007; Ravindra et al., 2008; Shih et al., 2008). The late onset of TCRV-induced apoptosis indicated that down-stream steps in virus replication (e.g. viral replication/transcription and/or the accumulation of viral RNA/proteins in the cytoplasm) were most likely responsible for the activation of apoptosis. Interestingly, the TCRV Z protein was shown to induce caspase 3 cleavage and chromatin condensation, suggesting that the accumulation of Z during infection might be a major factor contributing to the induction of apoptosis.

Further, we observed that, while TCRV infection induces cleavage of both caspases 8 and 9, the vast majority of signalling was via the intrinsic pathway (caspase 9). For many viruses like SeV, West Nile virus, Crimean-Congo hemorrhagic fever virus, Simian varicella virus, transmissible gastroenteritis virus or human astrovirus, it has been demonstrated that infection of the host cell can lead to activation of both caspases 8 and 9 and their associated signal transduction pathways (Banos-Lara Mdel & Mendez, 2010; Bitzer *et al.*, 2002; Bitzer *et al.*, 1999; Eleouet *et al.*, 1998; Kleinschmidt *et al.*, 2007; Pugazhenthi *et al.*, 2009; Rodrigues *et al.*, 2013). The exact

mechanism(s) by which these signalling pathways are activated during TCRV infection, and which cellular factors are involved, remains to be analysed. Most often PKR activation takes place during viral infection, activating apoptosis via the extrinsic (caspase 8) and the intrinsic (caspase 9) pathway. The activation of caspase 8 is, in this case, independent from death receptors on the cell surface (Balachandran *et al.*, 1998; Gil & Esteban, 2000; Iordanov *et al.*, 2005). Kolokoltsova and colleagues showed JUNV-induced apoptosis in HuH7 and A549 cells, which was RIG-I-dependent and IFN-I independent (Kolokoltsova *et al.*, 2014), an observation that is consistent with the finding that some RNA viruses can trigger mitochondrial apoptosis via a RIG-I/MAVS-dependent pathway involving IRF3 (Chattopadhyay *et al.*, 2010; Chattopadhyay *et al.*, 2011), and indeed this might also be the case for TCRV. However, whether apoptosis in TCRV infected cells is mediated by PKR, RIG-I/MAVS, other apoptotic sensors or additional caspase-independent signalling pathways, remains to be further determined.

TCRV-induced caspase activation could be observed in infected primary human macrophages, in HuH7 cells, and in IFN-defective VeroE6 cells (Desmyter *et al.*, 1968). Interestingly, the different cell types not only showed different susceptibility to TCRV infection, but also different degrees of sensitivity to apoptosis induction after either CPT-treatment or TCRV infection. TCRV-induced apoptotic signalling was particularly strong in primary human macrophages, which underlines the biological relevance of our findings, as these cells are important primary targets for arenavirus infection. Taken together, these data show that TCRV-induced apoptotic signalling can be observed in a variety of different mammalian cell types and does not seem to be dependent on the IFN competence of the cells. Based on recent findings, which suggest that the natural reservoir hosts of TCRV are ticks and bats (Downs *et al.*, 1963; Sayler *et al.*, 2014), it is necessary to extend the present analyses of primate cells to cells from the natural hosts. This will give valuable insights into how the host switch of TCRV changed the response of the infected cell in view of regulation of apoptosis.

Interestingly, the new data presented here, indicate that the closely related arenavirus species JUNV and TCRV use different strategies to modulate apoptosis in the infected host cell. In our previous work we could demonstrate an anti-apoptotic effect mediated by the highly pathogenic JUNV, which was based on a decoy function in which NP is cleaved by active caspases. However, while JUNV and TCRV NP show 78% identity at the amino acid level, further characterisation of JUNV and TCRV NP function has revealed that NP of the non-pathogenic TCRV showed neither a comparable specific pattern of NP cleavage, nor an apoptosis-suppressing influence. Consistent with these observations, TCRV induced significant hallmarks

of apoptosis during infection, while induction of apoptotic signalling by JUNV seems to be much weaker. Unlike for TCRV, we were unable to detect apoptosis induction by JUNV with IFA and Western blot analyses of infected VeroE6 cells. Only the more sensitive Caspase-Glo Assay revealed caspase activation in VeroE6 cells, as well as in primary human macrophages, during JUNV infection, and again caspase activation was much weaker in comparison to TCRV infected cells. Kolokoltsova et al. could further show JUNV-induced DNA fragmentation via ELISA, indicating that JUNV infection is also inducing apoptotic cell death. Interestingly, the degree of apoptosis also differed between JUNV Romero and Candid#1 in different cell lines (Kolokoltsova *et al.*, 2014). Clearly, further analyses, comparing apoptosis mechanisms between New World and Old World arenaviruses, as well as studies aimed at identifying the sensors involved in triggering apoptosis are needed, and would be of strong interest for the field.

Despite such an obvious difference with respect to the extent of apoptosis induction and the availability of inhibition mechanisms, in many cases TCRV and JUNV both show similar growth kinetics and comparable virus titres, indicating that apoptosis induction imparts no significant disadvantage for TCRV growth *in vitro*. This was confirmed by the observation that inhibition of caspases using Z-VAD-FMK did not have a positive effect on TCRV virus titres, while in contrast caspase activation seemed to contribute slightly to efficient viral growth. Thus, it remains unclear whether the absence of NP-cleavage, and its corresponding anti-apoptotic effect, presents a disadvantage for TCRV during infection. Whether TCRV actively exploits the apoptotic processes to support efficient virus replication and/or release and, if so, by which mechanism, also still needs to be determined. A positive influence of apoptosis induction in promoting viral growth or viral replication has been observed for many other viruses (Best *et al.*, 2003; Mendez *et al.*, 2004; Olsen *et al.*, 1996; Wurzer *et al.*, 2003). In those cases apoptotic processes help to overcome the host's immune response or facilitate viral entry or release (Amara & Mercer, 2015; Best *et al.*, 2003; Gliedman *et al.*, 1975; Jeurissen *et al.*, 1992; Teodoro & Branton, 1997). It is therefore tempting to speculate that the need for apoptosis induction during TCRV infection, but not JUNV infection, may be related to previously reported differences in the budding of these two viruses (Groseth *et al.*, 2010b; Wolff *et al.*, 2013b), and particularly the proline-rich domain-independent nature of TCRV budding (Urata *et al.*, 2009). While budding of viral particles is mediated by JUNV Z via its proline-rich late domains, TCRV Z is lacking any proline-rich late domain and only has a low budding activity when single expressed (Groseth *et al.*, 2010b). However, TCRV budding has been shown to be enhanced by the expression of additional viral proteins (i.e. NP), and the same may well be true for as yet unidentified cellular factors. Further, while virus-induced apoptosis does not play a role in the control of TCRV infection *in vitro*,

apoptotic processes might well be important at an organismal level for instance via immune-mediated mechanisms. Thus, the extent to which these two viruses are able to induce apoptosis during infection may still help in future to explain why JUNV and TCRV differ so dramatically in their pathogenicity, as well as to help predict the virulence of newly emerging arenavirus species.

Materials and Methods

Viruses and cell lines

TCRV (TRVL 11573) was kindly provided by Dan Kolakofsky (University of Geneva) and JUNV (Romero) was kindly provided by the Public Health Agency of Canada. Arenavirus stocks were prepared as previously described (Groseth *et al.*, 2010b). SeV was kindly provided by Marianne Nain (Philipps-University Marburg) and vesicular stomatitis virus (VSV, Indiana) was kindly provided by Friedemann Weber (Philipps-University Marburg). The experiments including JUNV were carried out in the biosafety level 4 (BSL-4) laboratory at the Philipps-University Marburg.

HuH7 (human hepatoma) and VeroE6 (African green monkey kidney) cells were cultured as previously described (Wolff *et al.*, 2013a). For isolation of primary human macrophages, leucocyte-enriched buffy coats from healthy anonymous donors were obtained from the blood bank of the Marburg-Gießen University Hospital. Samples were layered onto 13 ml of Lymphocyte Separation Medium (Pancoll density 1.077 g/ml, PAN Biotech) in a 50 ml tube. The blood was centrifuged at 670 *x g* for 30 min at room temperature (RT) with no brake. The layer formed by the mononuclear cells was carefully removed and washed twice with 50 ml of ice-cold PBS (-Mg/-Ca). After each washing step the cells were spun down at 350 *x g* for 10 min at 4°C with no brake. After the second centrifugation, the cells were resuspended in 20 ml RPMI-1640 media (Life Technologies). Monocytes were separated from the cell suspension by elutriation and resuspended in RPMI-1640 media with 5% human AB serum (Sigma) and seeded into Primaria 24-well ($7.5x10^5$ cells) or 96-well ($1.5x10^5$ cells) plates (BD Biosciences) and incubated at 37°C and 5% CO_2. After 1 h, the medium was removed and the cells were thoroughly washed twice with PBS (+Mg/+Ca) to remove non-attached cells. Then RPMI-1640 with 2% human AB serum was added to the cells, and they were incubated for differentiation into macrophages for 7 days at 37°C and 5% CO_2 before use.

Virus infection for apoptosis induction

Cell monolayers with a confluence of 60-80% were infected in 12-, 24- or 96-well plates (Greiner) with TCRV, JUNV (at an MOI of 1 or 3), SeV (20 HA /ml) or VSV (MOI 0.01) in serum-free DMEM at 37°C. After 1 h the inoculum was removed and the cells were placed in fresh DMEM containing 2% FBS, 2 mM L-glutamine, 100 U/ml penicillin and 100 µg/ml streptomycin. For macrophages fresh RPMI-1640 with 2% human AB serum was used instead. At the indicated time points p.i. cells were collected for further analysis.

Growth kinetics of TCRV in VeroE6 cells

VeroE6 cell monolayers at 80-90% confluence were infected with TCRV in 12-well plates (MOI 0.1) in 500 µl of serum-free DMEM for 1 h at 37°C in a 5% CO_2 atmosphere. Following absorption, the inoculum was removed and the cells were placed in fresh DMEM containing 2% FBS, 2 mM L-glutamine, 100 U/ml penicillin, and 100 µg/ml streptomycin and incubated for 6 days. Samples were collected every 24 h for analysis of progeny virus release by plaque assay as previously described (Wolff *et al.*, 2013a).

Treatment of cells for caspase inhibition or activation

For caspase inhibition the inhibitor Z-VAD-FMK (Promega) was added to the media to a final concentration of 50 µM. In addition, fresh Z-VAD-FMK in DMSO was added daily (20 µM). As a control, cells were treated with the same amount of DMSO. For caspase activation, CPT was used at final concentrations of 0.5 µM to 10 µM, as indicated. Except for growth kinetics, where supernatant was collected up to day 3 p.i., CPT-treated cells were analysed 24 h after treatment.

Inactivation of arenaviruses by UV irradiation

Stock preparations of TCRV with a titre of $1.5x10^6$ pfu/ml were inactivated as previously described (Carter *et al.*, 1973; Elliott *et al.*, 1982; Groseth *et al.*, 2010a) by irradiation at 254 nm using a UV Lamp (CAMAG) for 1 h. Inactivated samples were analysed by plaque assay as described previously (Wolff *et al.*, 2013a), to ensure complete inactivation (data not shown).

Western blot analysis

Western blot analysis was performed as previously described (Wolff *et al.*, 2013a). For detection, TCRV NP and JUNV NP specific antibodies (guinea pig) at a dilution of 1:500, and a secondary rabbit anti-guinea pig antibody conjugated to horseradish peroxidase (Dako, 1:30,000 dilution) were used. Tubulin and vinculin were detected using mouse monoclonal antibodies (Sigma-Aldrich, 1:5,000 dilution) and a secondary goat anti-mouse antibody conjugated to horseradish peroxidase (Dako, 1:30,000 dilution). For detection of caspases and PARP, a rabbit anti-caspase 3 antibody, a mouse anti-caspase 8 antibody, a mouse anti-caspase 9 antibody and a rabbit anti-PARP antibody (all from Cell Signalling) were used at a dilution of 1:1,000 and a secondary swine anti-rabbit antibody or a goat anti-mouse antibody conjugated to horseradish peroxidase (Dako, 1:30,000 dilution) were used for detection. For detection of Flag-tagged constructs, a monoclonal M2 mouse anti-Flag antibody (Sigma-Aldrich, 1:1,000 dilution) and a goat anti-mouse antibody conjugated to horseradish peroxidase (Dako, 1:30,000 dilution) were used. Signals were detected and quantified using the Chemi Doc XRS+ System (Bio-Rad) with the Image Lab software (Version 4.0).

Microscopic and immunofluorescence analysis

Immunofluorescence analysis was performed as previously described (Wolff *et al.*, 2013a) at the indicated time points. For staining of the nuclei, cells were incubated for 1 h with DAPI (Sigma-Aldrich, 1:20,000 dilution). For detection of TCRV NP, a TCRV NP specific antibody (guinea pig) at a dilution of 1:100 and a secondary Alexa488 coupled goat anti-guinea pig antibody (Molecular Probes, dilution of 1:500) were used.

Caspase-Glo Assays

For the Caspase-Glo 3/7, 8, and 9 Assays (Promega) cell monolayers with a confluence of 30% were seeded in a 96-well plate format and infected with TCRV, JUNV (at an MOI of 1 or 3), VSV (at an MOI 0.01) or SeV (final concentration 20 HA/ml) for 1 h at 37°C in a 5% CO_2 atmosphere in serum-free DMEM. Following absorption, the inoculum was removed and the cells were placed in 100 µl fresh DMEM containing 3% FBS, 2 mM L-glutamine, 100 U/ml penicillin, and 100 µg/ml streptomycin. At the indicated time points samples were processed according to the manufacturer's instructions. Briefly, a single Caspase-Glo® Reagent, containing a proluminescent substrate for caspase 3/7, 8 or 9, was added, resulting in cell lysis, substrate cleavage by activated caspases and the release of aminoluciferin, a substrate of luciferase used in light production. The luminescent signal was measured using a Luminometer Centro LB 960.

Transfection of virus proteins

For expression of the TCRV proteins, transfection into VeroE6 cells (60% confluent) was carried out using TransIT-LT1 (Mirus) according to the manufacturer's instructions using 3 µl TransIT per µg DNA. Here 1 µg per well (6-well, Greiner) of each plasmid was used. Cell lysates were harvested for Western blot analysis at 48 h p.t..

Statistical analysis

The presented data for most experiments, as indicated, represent the mean value and standard deviation of at least three independent experiments. The statistical significance was determined using one-way ANOVA tests (Microsoft Excel, XL toolbar), as indicated. Asterisks indicate statistically significant differences (*$p<0.05$, **$p<0.01$, ***$p<0.001$).

Acknowledgements

The authors are very grateful to Verena Krähling, Thomas Hoenen, Sarah Fehling, Logan Banadyga and Sonja Best for their helpful discussion and suggestions. We also wish to thank Astrid Herwig, Katharina Kowalski and Dirk Becker for their excellent technical assistance and Markus Eickmann, Gotthard Ludwig and Michael Schmidt for their technical assistance with the BSL-4 laboratory.

This work was supported in part by fellowships from the Jürgen Manchot Stiftung (SW; http://www.manchot.org), the German Research Council (SFB 1021 TP A04 (AK), B03 (SB, SW) and B05 (TS); http://www.uni-marburg.de/sfb1021), the Canadian Institutes of Health Research (AG; http://www.cihr-irsc.gc.ca) and a Medical Research Council Centenary Travel Award (BM). This research was also supported in part by the Philipps-University Marburg.

References

Abraham, J., Kwong, J. A., Albarino, C. G., Lu, J. G., Radoshitzky, S. R., Salazar-Bravo, J., Farzan, M., Spiropoulou, C. F. & Choe, H. (2009). Host-species transferrin receptor 1 orthologs are cellular receptors for nonpathogenic new world clade B arenaviruses. *PLoS Pathog* **5**, e1000358.

Acrani, G. O., Gomes, R., Proenca-Modena, J. L., da Silva, A. F., Carminati, P. O., Silva, M. L., Santos, R. I. & Arruda, E. (2009). Apoptosis induced by Oropouche virus infection in HeLa cells is dependent on virus protein expression. *Virus Res* **149**, 56-63.

Amara, A. & Mercer, J. (2015). Viral apoptotic mimicry. *Nat Rev Microbiol* **13**, 461-469.

Ashkenazi, A. & Dixit, V. M. (1998). Death receptors: signaling and modulation. *Science* **281**, 1305-1308.

Balachandran, S., Kim, C. N., Yeh, W. C., Mak, T. W., Bhalla, K. & Barber, G. N. (1998). Activation of the dsRNA-dependent protein kinase, PKR, induces apoptosis through FADD-mediated death signaling. *EMBO J* **17**, 6888-6902.

Banos-Lara Mdel, R. & Mendez, E. (2010). Role of individual caspases induced by astrovirus on the processing of its structural protein and its release from the cell through a non-lytic mechanism. *Virology* **401**, 322-332.

Best, S. M., Shelton, J. F., Pompey, J. M., Wolfinbarger, J. B. & Bloom, M. E. (2003). Caspase cleavage of the nonstructural protein NS1 mediates replication of Aleutian mink disease parvovirus. *J Virol* **77**, 5305-5312.

Bitzer, M., Armeanu, S., Prinz, F., Ungerechts, G., Wybranietz, W., Spiegel, M., Bernlohr, C., Cecconi, F., Gregor, M., Neubert, W. J., Schulze-Osthoff, K. & Lauer, U. M. (2002). Caspase-8 and Apaf-1-independent caspase-9 activation in Sendai virus-infected cells. *J Biol Chem* **277**, 29817-29824.

Bitzer, M., Prinz, F., Bauer, M., Spiegel, M., Neubert, W. J., Gregor, M., Schulze-Osthoff, K. & Lauer, U. (1999). Sendai virus infection induces apoptosis through activation of caspase-8 (FLICE) and caspase-3 (CPP32). *J Virol* **73**, 702-708.

Borner, C. & Monney, L. (1999). Apoptosis without caspases: an inefficient molecular guillotine? *Cell Death Differ* **6**, 497-507.

Briese, T., Paweska, J. T., McMullan, L. K., Hutchison, S. K., Street, C., Palacios, G., Khristova, M. L., Weyer, J., Swanepoel, R., Egholm, M., Nichol, S. T. & Lipkin, W. I. (2009). Genetic detection and characterization of Lujo virus, a new hemorrhagic fever-associated arenavirus from southern Africa. *PLoS Pathog* **5**, e1000455.

Cande, C., Cecconi, F., Dessen, P. & Kroemer, G. (2002). Apoptosis-inducing factor (AIF): key to the conserved caspase-independent pathways of cell death? *J Cell Sci* **115**, 4727-4734.

Carballal, G., Calello, M. A., Laguens, R. P. & Weissenbacher, M. C. (1987). Tacaribe virus: a new alternative for Argentine hemorrhagic fever vaccine. *J Med Virol* **23**, 257-263.

Carter, M. F., Murphy, F. A., Brunschwig, J. P., Noonan, C. & Rawls, W. E. (1973). Effects of actinomycin D and ultraviolet and ionizing radiation on Pichinde virus. *J Virol* **12**, 33-38.

Chattopadhyay, S., Marques, J. T., Yamashita, M., Peters, K. L., Smith, K., Desai, A., Williams, B. R. & Sen, G. C. (2010). Viral apoptosis is induced by IRF-3-mediated activation of Bax. *EMBO J* **29**, 1762-1773.

Chattopadhyay, S., Yamashita, M., Zhang, Y. & Sen, G. C. (2011). The IRF-3/Bax-mediated apoptotic pathway, activated by viral cytoplasmic RNA and DNA, inhibits virus replication. *J Virol* **85**, 3708-3716.

Daugas, E., Nochy, D., Ravagnan, L., Loeffler, M., Susin, S. A., Zamzami, N. & Kroemer, G. (2000). Apoptosis-inducing factor (AIF): a ubiquitous mitochondrial oxidoreductase involved in apoptosis. *FEBS Lett* **476**, 118-123.

548 **Desmyter, J., Melnick, J. L. & Rawls, W. E. (1968).** Defectiveness of interferon production and
549 of rubella virus interference in a line of African green monkey kidney cells (Vero). *J Virol*
550 **2**, 955-961.
551 **Downs, W. G., Anderson, C. R., Spence, L., Aitken, T. H. & Greenhall, A. H. (1963).** Tacaribe
552 virus, a new agent isolated from Artibeus bats and mosquitoes in Trinidad, West Indies.
553 *Am J Trop Med Hyg* **12**, 640-646.
554 **Eleouet, J. F., Chilmonczyk, S., Besnardeau, L. & Laude, H. (1998).** Transmissible
555 gastroenteritis coronavirus induces programmed cell death in infected cells through a
556 caspase-dependent pathway. *J Virol* **72**, 4918-4924.
557 **Elliott, L. H., McCormick, J. B. & Johnson, K. M. (1982).** Inactivation of Lassa, Marburg, and
558 Ebola viruses by gamma irradiation. *Journal of clinical microbiology* **16**, 704-708.
559 **Fischer, U., Janicke, R. U. & Schulze-Osthoff, K. (2003).** Many cuts to ruin: a comprehensive
560 update of caspase substrates. *Cell Death Differ* **10**, 76-100.
561 **Gadaleta, P., Vacotto, M. & Coulombie, F. (2002).** Vesicular stomatitis virus induces apoptosis
562 at early stages in the viral cycle and does not depend on virus replication. *Virus Res* **86**,
563 87-92.
564 **Gil, J. & Esteban, M. (2000).** The interferon-induced protein kinase (PKR), triggers apoptosis
565 through FADD-mediated activation of caspase 8 in a manner independent of Fas and
566 TNF-alpha receptors. *Oncogene* **19**, 3665-3674.
567 **Gliedman, J. B., Smith, J. F. & Brown, D. T. (1975).** Morphogenesis of Sindbis virus in cultured
568 Aedes albopictus cells. *J Virol* **16**, 913-926.
569 **Granville, D. J. & Gottlieb, R. A. (2002).** Mitochondria: regulators of cell death and survival.
570 *ScientificWorldJournal* **2**, 1569-1578.
571 **Green, D. & Kroemer, G. (1998).** The central executioners of apoptosis: caspases or
572 mitochondria? *Trends Cell Biol* **8**, 267-271.
573 **Groseth, A., Hoenen, T., Weber, M., Wolff, S., Herwig, A., Kaufmann, A. & Becker, S.**
574 **(2010a).** Tacaribe virus but not junin virus infection induces cytokine release from
575 primary human monocytes and macrophages. *PLoS Negl Trop Dis* **5**, e1137.
576 **Groseth, A., Wolff, S., Strecker, T., Hoenen, T. & Becker, S. (2010b).** Efficient budding of the
577 tacaribe virus matrix protein z requires the nucleoprotein. *J Virol* **84**, 3603-3611.
578 **Hay, S. & Kannourakis, G. (2002).** A time to kill: viral manipulation of the cell death program. *J*
579 *Gen Virol* **83**, 1547-1564.
580 **Ho, P. K. & Hawkins, C. J. (2005).** Mammalian initiator apoptotic caspases. *FEBS J* **272**, 5436-
581 5453.
582 **Iordanov, M. S., Kirsch, J. D., Ryabinina, O. P., Wong, J., Spitz, P. N., Korcheva, V. B.,**
583 **Thorburn, A. & Magun, B. E. (2005).** Recruitment of TRADD, FADD, and caspase 8 to
584 double-stranded RNA-triggered death inducing signaling complexes (dsRNA-DISCs).
585 *Apoptosis : an international journal on programmed cell death* **10**, 167-176.
586 **Ivana Scovassi, A. & Diederich, M. (2004).** Modulation of poly(ADP-ribosylation) in apoptotic
587 cells. *Biochemical pharmacology* **68**, 1041-1047.
588 **Jeurissen, S. H., Wagenaar, F., Pol, J. M., van der Eb, A. J. & Noteborn, M. H. (1992).**
589 Chicken anemia virus causes apoptosis of thymocytes after in vivo infection and of cell
590 lines after in vitro infection. *J Virol* **66**, 7383-7388.
591 **Karlberg, H., Tan, Y. J. & Mirazimi, A. (2010).** Induction of caspase activation and cleavage of
592 the viral nucleocapsid protein in different cell types during Crimean-Congo hemorrhagic
593 fever virus infection. *J Biol Chem* **286**, 3227-3234.
594 **King, A. M. Q., Adams, M.J., Carstens, E.B. and Lefkowitz, E.J. (2009).** Virus taxonomy:
595 classification and nomenclature of viruses: Ninth Report of the International Committee
596 on Taxonomy of Viruses. *Elsevier*.
597 **Kleinschmidt, M. C., Michaelis, M., Ogbomo, H., Doerr, H. W. & Cinatl, J., Jr. (2007).**
598 Inhibition of apoptosis prevents West Nile virus induced cell death. *BMC Microbiol* **7**, 49.

Kolokoltsova, O. A., Grant, A. M., Huang, C., Smith, J. K., Poussard, A. L., Tian, B., Brasier, A. R., Peters, C. J., Tseng, C. T., de la Torre, J. C. & Paessler, S. (2014). RIG-I enhanced interferon independent apoptosis upon Junin virus infection. *PLoS One* **9**, e99610.

Kumar, S. (2007). Caspase function in programmed cell death. *Cell Death Differ* **14**, 32-43.

Li, X. D., Kukkonen, S., Vapalahti, O., Plyusnin, A., Lankinen, H. & Vaheri, A. (2004). Tula hantavirus infection of Vero E6 cells induces apoptosis involving caspase 8 activation. *J Gen Virol* **85**, 3261-3268.

Mendez, E., Salas-Ocampo, E. & Arias, C. F. (2004). Caspases mediate processing of the capsid precursor and cell release of human astroviruses. *J Virol* **78**, 8601-8608.

Nunez, G., Benedict, M. A., Hu, Y. & Inohara, N. (1998). Caspases: the proteases of the apoptotic pathway. *Oncogene* **17**, 3237-3245.

Olsen, C. W., Kehren, J. C., Dybdahl-Sissoko, N. R. & Hinshaw, V. S. (1996). bcl-2 alters influenza virus yield, spread, and hemagglutinin glycosylation. *J Virol* **70**, 663-666.

Peters, C. J., Buchmeier, M., Rollin, P.E., Ksiazek, T.G. (1996). Arenaviruses. *Fields Virology 3rd ed Lippincott-Raven Publishers, Philadelphia, PA:pp 1521-1551*

Pugazhenthi, S., Gilden, D. H., Nair, S., McAdoo, A., Wellish, M., Brazeau, E. & Mahalingam, R. (2009). Simian varicella virus induces apoptosis in monkey kidney cells by the intrinsic pathway and involves downregulation of bcl-2 expression. *J Virol* **83**, 9273-9282.

Ravindra, P. V., Tiwari, A. K., Ratta, B., Chaturvedi, U., Palia, S. K., Subudhi, P. K., Kumar, R., Sharma, B., Rai, A. & Chauhan, R. S. (2008). Induction of apoptosis in Vero cells by Newcastle disease virus requires viral replication, de-novo protein synthesis and caspase activation. *Virus Res* **133**, 285-290.

Richard, A. & Tulasne, D. (2012). Caspase cleavage of viral proteins, another way for viruses to make the best of apoptosis. *Cell Death Dis* **3**, e277.

Rodrigues, R., Paranhos-Baccala, G., Vernet, G. & Peyrefitte, C. N. (2013). Crimean-Congo hemorrhagic fever virus-infected hepatocytes induce ER-stress and apoptosis crosstalk. *PLoS One* **7**, e29712.

Roulston, A., Marcellus, R. C. & Branton, P. E. (1999). Viruses and apoptosis. *Annu Rev Microbiol* **53**, 577-628.

Sayler, K. A., Barbet, A. F., Chamberlain, C., Clapp, W. L., Alleman, R., Loeb, J. C. & Lednicky, J. A. (2014). Isolation of Tacaribe virus, a Caribbean arenavirus, from host-seeking Amblyomma americanum ticks in Florida. *PLoS One* **9**, e115769.

Shih, S. R., Weng, K. F., Stollar, V. & Li, M. L. (2008). Viral protein synthesis is required for Enterovirus 71 to induce apoptosis in human glioblastoma cells. *J Neurovirol* **14**, 53-61.

Teodoro, J. G. & Branton, P. E. (1997). Regulation of apoptosis by viral gene products. *J Virol* **71**, 1739-1746.

Thompson, M. R., Kaminski, J. J., Kurt-Jones, E. A. & Fitzgerald, K. A. (2011). Pattern recognition receptors and the innate immune response to viral infection. *Viruses* **3**, 920-940.

Timmer, J. C. & Salvesen, G. S. (2007). Caspase substrates. *Cell Death Differ* **14**, 66-72.

Urata, S., Yasuda, J. & de la Torre, J. C. (2009). The z protein of the new world arenavirus tacaribe virus has bona fide budding activity that does not depend on known late domain motifs. *J Virol* **83**, 12651-12655.

Weissenbacher, M. C., Coto, C. E. & Calello, M. A. (1975). Cross-protection between Tacaribe complex viruses. Presence of neutralizing antibodies against Junin virus (Argentine hemorrhagic fever) in guinea pigs infected with Tacaribe virus. *Intervirology* **6**, 42-49.

Wolff, S., Becker, S. & Groseth, A. (2013a). Cleavage of the Junin virus nucleoprotein serves a decoy function to inhibit the induction of apoptosis during infection. *J Virol* **87**, 224-233.

Wolff, S., Ebihara, H. & Groseth, A. (2013b). Arenavirus budding: a common pathway with mechanistic differences. *Viruses* **5**, 528-549.

Wurzer, W. J., Planz, O., Ehrhardt, C., Giner, M., Silberzahn, T., Pleschka, S. & Ludwig, S. (2003). Caspase 3 activation is essential for efficient influenza virus propagation. *EMBO J* **22**, 2717-2728.

Xing, J., Ly, H. & Liang, Y. (2015). The Z proteins of pathogenic but not nonpathogenic arenaviruses inhibit RIG-I-like receptor-dependent interferon production. *J Virol* **89**, 2944-2955.

Figure Legends

Fig. 1: TCRV infection induces apoptosis in VeroE6 cells.

(a) Caspase 3 cleavage during TCRV infection. VeroE6 cells were infected with TCRV at an MOI of 1 or with SeV (20 HA/ml) as a positive control for apoptosis induction. The cell lysates were collected and analysed by SDS-PAGE and Western blot at the indicated time points. Samples were probed for TCRV NP expression, as well as caspase 3 and its cleavage product. Tubulin levels served as a loading control. **(b)** CPE formation and chromatin condensation during TCRV infection. VeroE6 cells were infected as described in (a). The CPE was monitored daily (shown here for days 1 to 3 p.i.). Afterwards the cells were fixed and the nuclei were stained with DAPI to visualize chromatin condensation (indicated by white arrows). The presented IFA and CPE images were taken using the same samples but are not of the same field. **(c)** Caspase 3/7 activation during TCRV infection. VeroE6 cells were infected with TCRV at an MOI of 1. The activity of caspases 3/7 was measured at the indicated time points using a Caspase-Glo 3/7 Assay. CPT-treated cells (10 µM) served as a control for the activation of apoptosis. Data represent the mean values and standard deviations of three independent replicates representative of three independent experiments. The statistical significance was determined using one-way ANOVA. Asterisks indicate statistically significant differences (*$p<0.05$, **$p<0.01$) in comparison to mock infected cells.

Fig. 2: TCRV-induced apoptosis depends on intracellular virus processes.

(a) CPE formation and chromatin condensation during infection with infectious and UV-inactivated TCRV. VeroE6 cells were infected with TCRV at an MOI of 1 and the same amount of UV-inactivated TCRV. CPE formation was monitored and the cells were fixed and nuclei were stained with DAPI to visualize chromatin condensation (shown here for day 3 and/or 6 p.i., as indicated). The confluent cell layer was further incubated with antibodies against TCRV NP for detection of viral antigen. The presented IFA and CPE images were taken using the same sample but are not of the same field. **(b)** Caspase 3 and PARP cleavage during infection with infectious or UV-inactivated TCRV and JUNV. VeroE6 cells were infected as described in (a). JUNV infection (MOI 3) served as additional control. The cell lysates were collected and analysed by SDS-PAGE and Western blot at the indicated time points. Samples were probed for TCRV NP and JUNV NP expression, as well as PARP and caspase 3 and their respective cleavage products. Tubulin levels served as a loading control. **(c)** Caspase 3/7 activation during infection with infectious and UV-inactivated TCRV and JUNV. VeroE6 cells were infected with TCRV or JUNV at an MOI of 1 and the same amount of UV-inactivated virus. CPT-treatment (10

693 µM) and VSV infection (MOI 0.01) served as additional controls. The activity of caspases 3/7
694 was measured at day 3 p.i. using a Caspase-Glo 3/7 Assay. Data represent the mean values
695 and standard deviations of three independent replicates representative of three independent
696 experiments. The statistical significance was determined using one-way ANOVA. Asterisks
697 indicate statistically significant differences (*p<0.05, **p<0.01). **(d)** VeroE6 cells were transfected
698 with constructs for expression of single TCRV proteins. CPE was monitored 48 h p.t. and the
699 cells were fixed and stained with DAPI to visualize chromatin condensation (indicated by white
700 arrows). The presented IFA and CPE images were taken using the same samples but are not of
701 the same field. **(e)** VeroE6 cells were transfected as described in (d) and 48 h p.t. cell lysates
702 were collected and analysed by SDS-PAGE and Western blot. Samples were probed for TCRV
703 protein expression, as well as caspase 3 and the respective cleavage product. CPT-treated cells
704 (5 µM) served as control.
705
706 **Fig. 3: TCRV infection activates caspases of the extrinsic and the intrinsic pathway.**
707 **(a)** Caspase 8 and 9 cleavage during TCRV infection. VeroE6 cells were infected with TCRV at
708 an MOI of 1 or treated with the same amount of UV-inactivated TCRV. Infection with SeV (20
709 HA/ml) served as positive control for the induction of both caspases 8 and 9. The cell lysates
710 were collected and analysed by SDS-PAGE and Western blot at the indicated time points.
711 Samples were probed for TCRV NP expression, as well as caspase 8 and 9 and their respective
712 cleavage products. **(b)** Caspase 8 and 9 activation during infection with infectious and UV-
713 inactivated TCRV. VeroE6 cells were infected with TCRV, UV-inactivated TCRV and SeV as
714 described in (a). The activity of caspases 8 and 9 was measured at day 3 p.i. (SeV day 1 p.i.)
715 using a Caspase-Glo Assay. Data represent the mean values and standard deviations of three
716 independent replicates representative of three independent experiments. The statistical
717 significance was determined using one-way ANOVA. Asterisks indicate statistically significant
718 differences (*p<0.05, **p<0.01, ***p<0.001).
719
720 **Fig. 4: TCRV-induced caspase activation in different cell types.**
721 **(a)** TCRV infection of HuH7, VeroE6 cells and primary human macrophages. The indicated cell
722 types were infected with TCRV at an MOI of 3. The CPE was monitored on day 3 p.i. and the
723 cell lysates were collected and analysed by SDS-PAGE and Western blot. Samples were probed
724 for expression of TCRV NP and vinculin as a loading control. **(b)** Caspase 3/7 activation in
725 TCRV infected HuH7, VeroE6 cells and primary human macrophages. The indicated cell types
726 were infected with TCRV with either an MOI of 1 or 3, as indicated, and analysed on day 3 p.i.
727 with a Caspase-Glo 3/7 Assay. CPT-treated cells served as a positive control for apoptosis

induction. For statistical analysis one-way ANOVA was used to analyse TCRV-dependent apoptosis induction within each cell line. Asterisks indicate statistically significant differences (*p<0.05, **p<0.01) in comparison to mock infected cells.

Fig. 5: Caspase activation in TCRV and JUNV infected primary human macrophages.
(a) JUNV and TCRV infection of primary human macrophages. Primary human macrophages from two different donors were infected with TCRV and JUNV at an MOI of 1. At 72 h p.i. CPE formation and NP-expression, to demonstrate the cells' susceptibility to arenavirus infection, were analysed. **(b)** Caspase activation in TCRV and JUNV infected primary human macrophages. Primary human macrophages from two different donors were infected with TCRV and JUNV at an MOI of 1 or the same amount of UV-inactivated virus as a control. The activity of caspases 3/7, 8, and 9 was measured on day 3 p.i. using separate Caspase-Glo Assays. CPT-treated (5 µM) macrophages were analysed after 24 h incubation with the Caspase-Glo 3/7 Assay and served as a control for the activation of apoptosis.

Fig. 6: TCRV growth is slightly affected by caspase activity in VeroE6 cells.
(a) TCRV infection in the presence of the caspase inhibitor Z-VAD-FMK. VeroE6 cells were infected with TCRV at an MOI of 0.1 and growth kinetics were performed from day 1 to day 6 p.i.. To analyse the effect of caspase activity on viral growth, cells were treated after infection with the caspase inhibitor Z-VAD-FMK (50 µM) or with DMSO as a control. To ensure stability of the inhibitor, Z-VAD-FMK (20 µM) or DMSO were added daily. CPE was monitored daily and supernatants were collected for titre determination via plaque assay. Data represent the mean values and standard deviations of three independent replicates representative of three independent experiments. **(b)** TCRV infection in the presence of the apoptosis inducer CPT. VeroE6 cells were infected as described in (a). To analyse the effect of enhanced caspase activity on viral growth, cells were additionally treated once with CPT (0.5 µM, 1 µM) after infection. The CPE was monitored daily (shown here for day 2 p.i.) and supernatants were collected every day for titre determination via plaque assay. Due to decreased cell viability, growth kinetics were only conducted up to day 3 p.i.. For comparison of TCRV titres at single time points, one-way ANOVA was used for statistical analysis. Asterisks indicate statistically significant differences (*p<0.05, **p<0.01).

Fig. 1

(a)

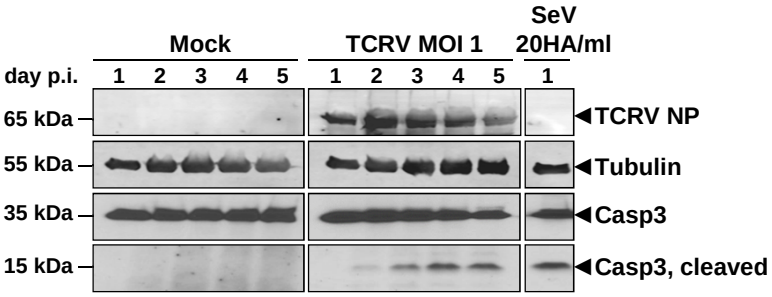
Mock
TCRV MOI 1
SeV 20HA/ml
day p.i.
1 2 3 4 5 1 2 3 4 5 1
65 kDa
55 kDa
35 kDa
15 kDa
TCRV NP
Tubulin
Casp3
Casp3, cleaved

(b)

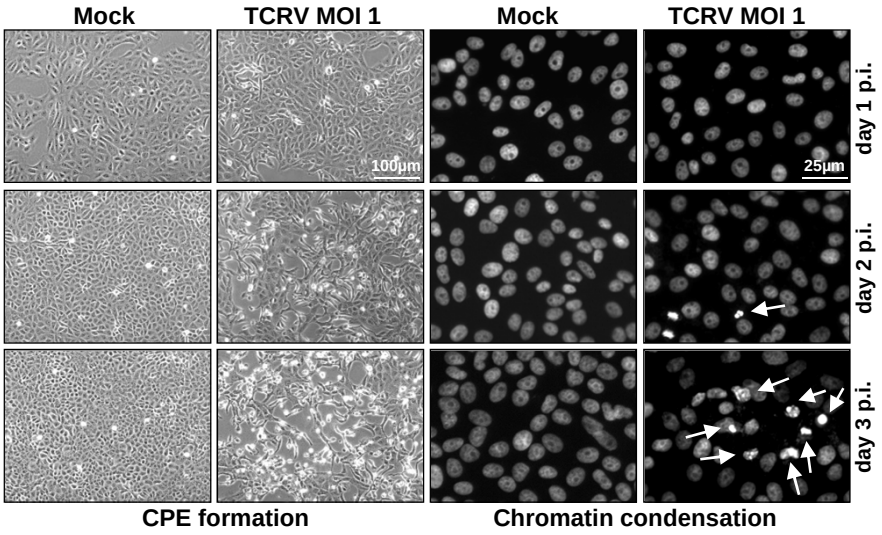
Mock
TCRV MOI 1
Mock
TCRV MOI 1
100µm
25µm
day 1 p.i.
day 2 p.i.
day 3 p.i.
CPE formation
Chromatin condensation

(c)

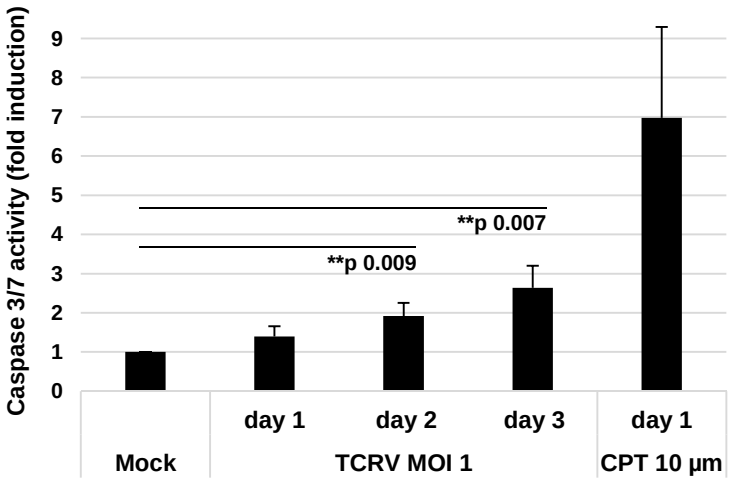
Caspase 3/7 activity (fold induction)
0
1
2
3
4
5
6
7
8
9
**p 0.009
**p 0.007
day 1
day 2
day 3
day 1
Mock
TCRV MOI 1
CPT 10 µm

Fig. 2

(a)

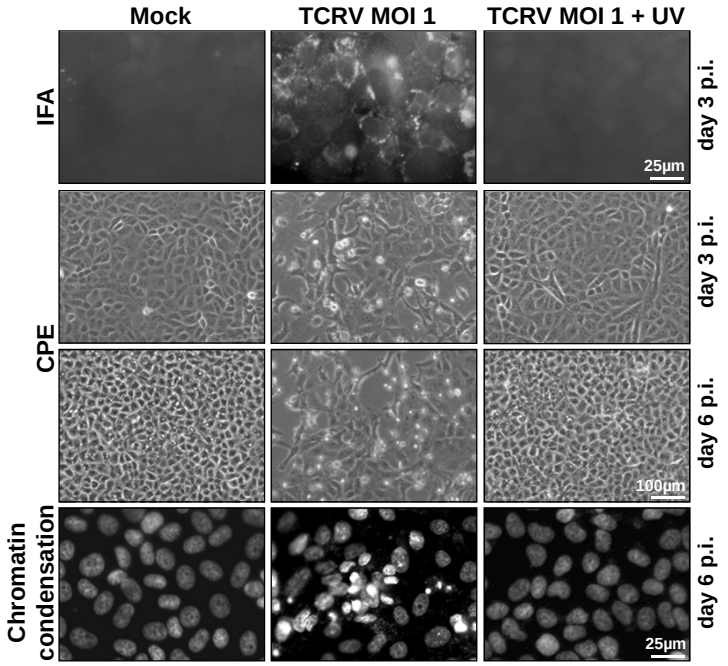
Mock
TCRV MOI 1
TCRV MOI 1 + UV
IFA
CPE
Chromatin condensation
day 3 p.i.
day 3 p.i.
day 6 p.i.
day 6 p.i.
25µm
100µm
25µm

(b)

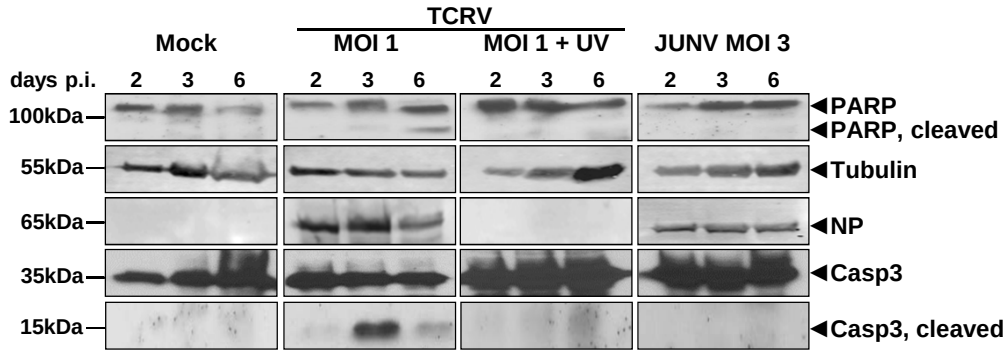
Mock
TCRV
MOI 1
MOI 1 + UV
JUNV MOI 3
days p.i. 2 3 6 2 3 6 2 3 6 2 3 6
100kDa
55kDa
65kDa
35kDa
15kDa
PARP
PARP, cleaved
Tubulin
NP
Casp3
Casp3, cleaved

(c)

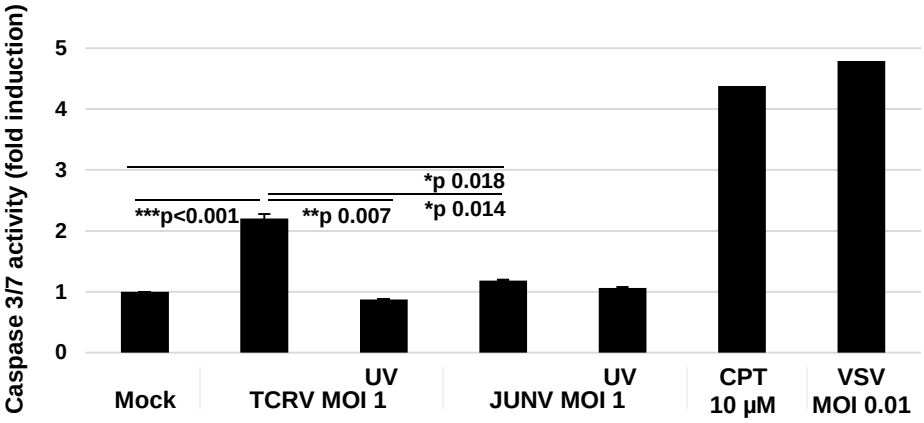
Caspase 3/7 activity (fold induction)
0
1
2
3
4
5
***p<0.001
**p 0.007
*p 0.018
*p 0.014
Mock
TCRV MOI 1
UV
JUNV MOI 1
UV
CPT 10 µM
VSV MOI 0.01

Fig. 2

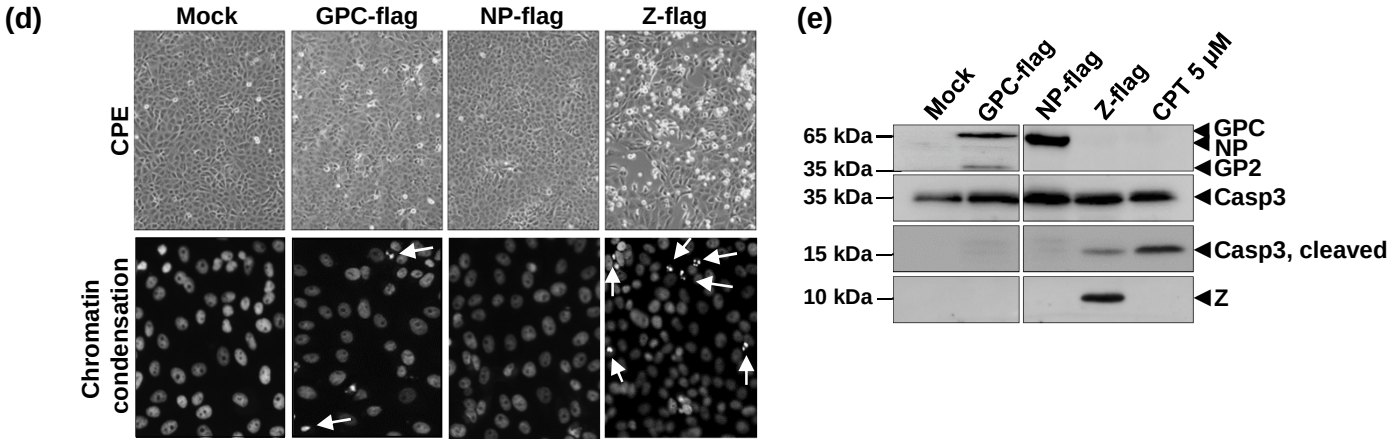
(d)
Mock
GPC-flag
NP-flag
Z-flag
CPE
Chromatin condensation
(e)
Mock
GPC-flag
NP-flag
Z-flag
CPT 5 μM
65 kDa
35 kDa
35 kDa
15 kDa
10 kDa
GPC
NP
GP2
Casp3
Casp3, cleaved
Z

Fig. 3

(a)

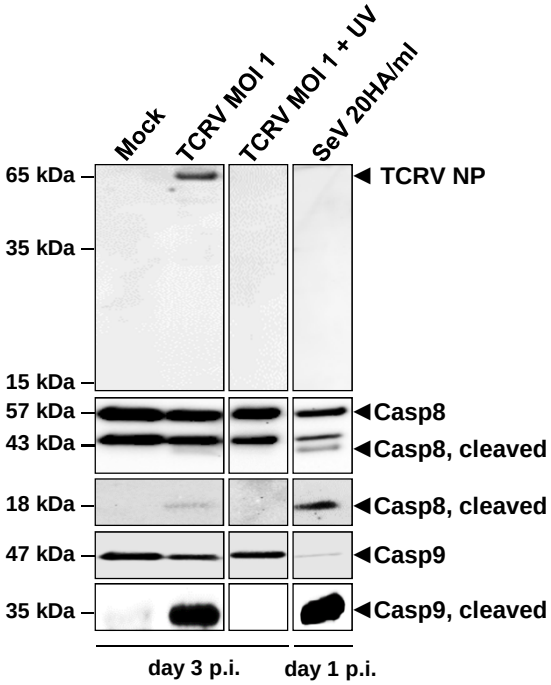
Mock
TCRV MOI 1
TCRV MOI 1 + UV
SeV 20HA/ml
65 kDa
35 kDa
15 kDa
TCRV NP
57 kDa
43 kDa
Casp8
Casp8, cleaved
18 kDa
Casp8, cleaved
47 kDa
Casp9
35 kDa
Casp9, cleaved
day 3 p.i.
day 1 p.i.

(b)

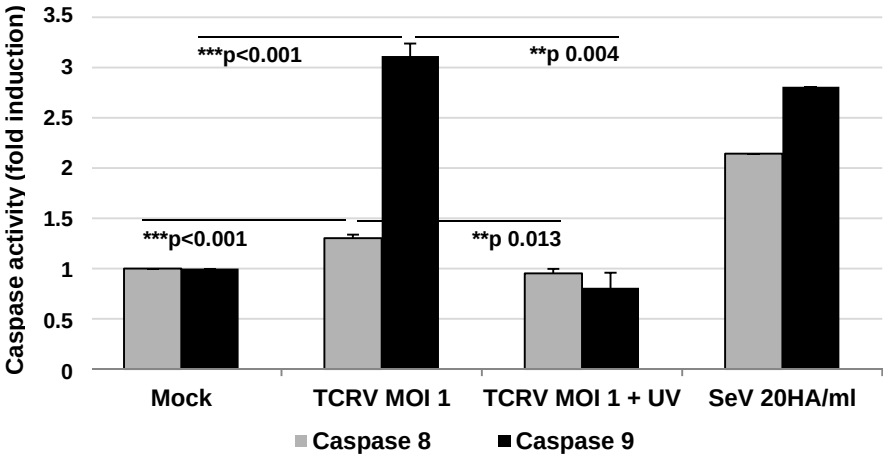
Caspase activity (fold induction)
3.5
3
2.5
2
1.5
1
0.5
0
***p<0.001
**p 0.004
***p<0.001
**p 0.013
Mock
TCRV MOI 1
TCRV MOI 1 + UV
SeV 20HA/ml
Caspase 8
Caspase 9

Fig. 4

(a)

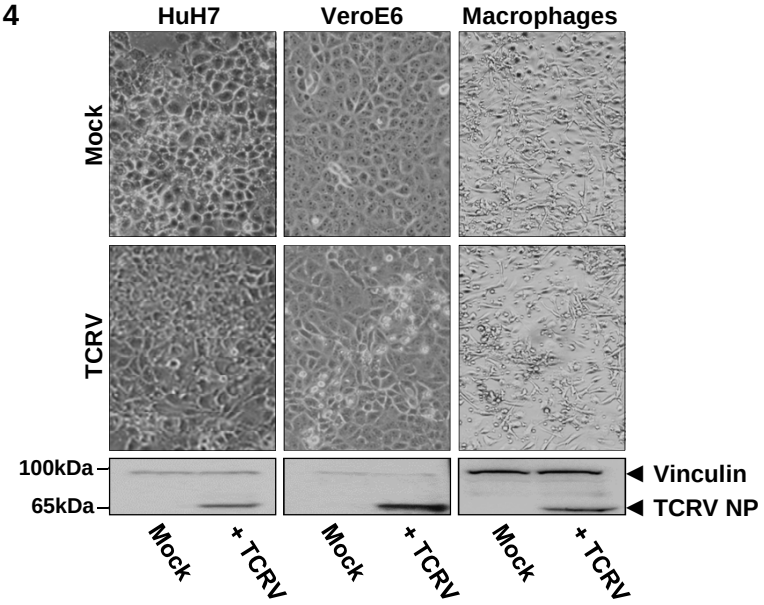
HuH7
VeroE6
Macrophages
Mock
TCRV
100kDa
65kDa
Vinculin
TCRV NP
Mock
+ TCRV
Mock
+ TCRV
Mock
+ TCRV

(b)

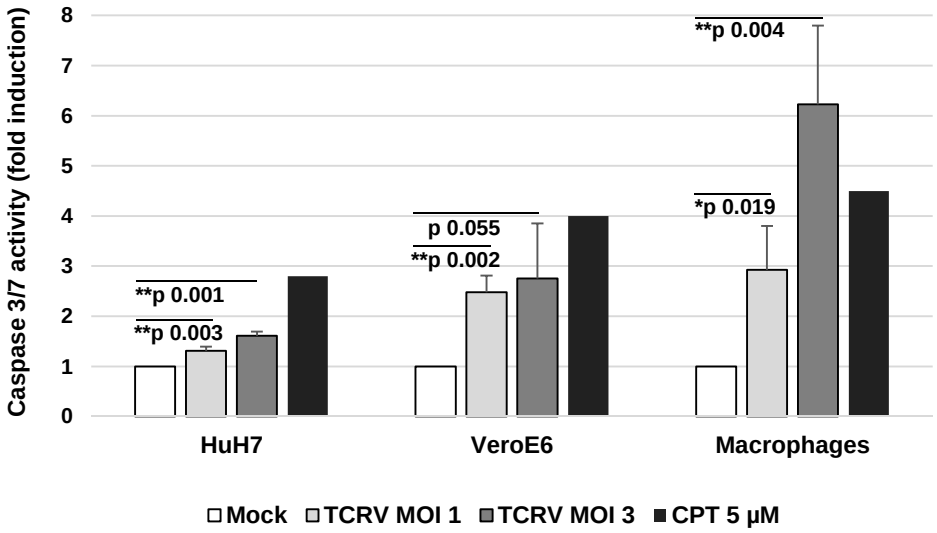
Caspase 3/7 activity (fold induction)
0
1
2
3
4
5
6
7
8
**p 0.001
**p 0.003
p 0.055
**p 0.002
**p 0.004
*p 0.019
HuH7
VeroE6
Macrophages
Mock
TCRV MOI 1
TCRV MOI 3
CPT 5 µM

Fig. 5

(a)

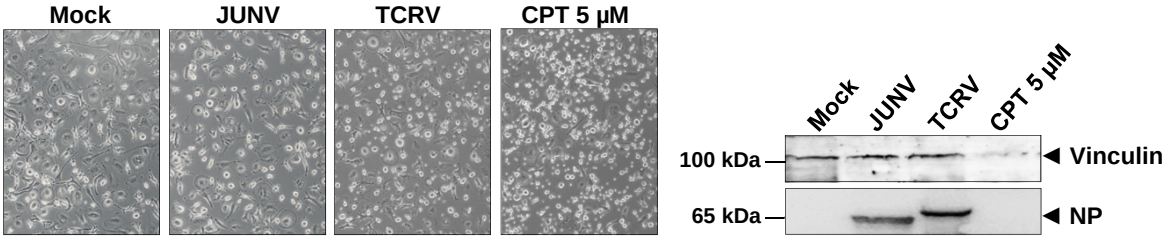
Mock
JUNV
TCRV
CPT 5 µM
Mock
JUNV
TCRV
CPT 5 µM
100 kDa
Vinculin
65 kDa
NP

(b)

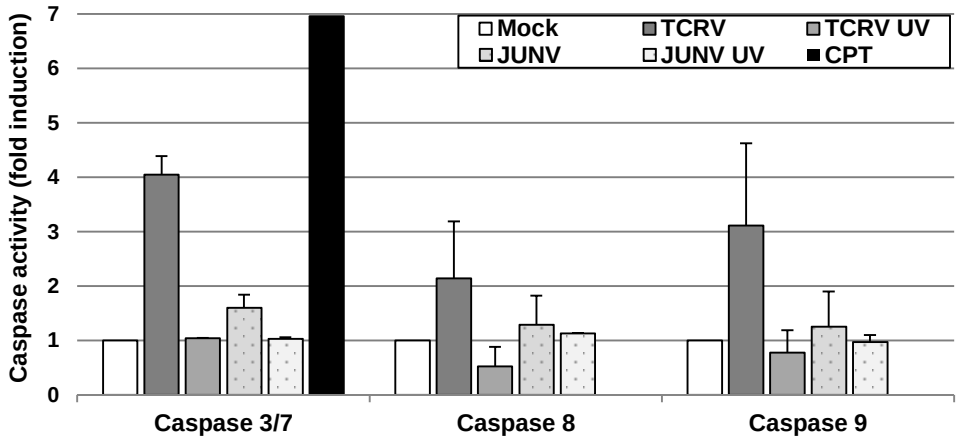
Caspase activity (fold induction)
0
1
2
3
4
5
6
7
Mock
TCRV
TCRV UV
JUNV
JUNV UV
CPT
Caspase 3/7
Caspase 8
Caspase 9

Fig. 6

(a)

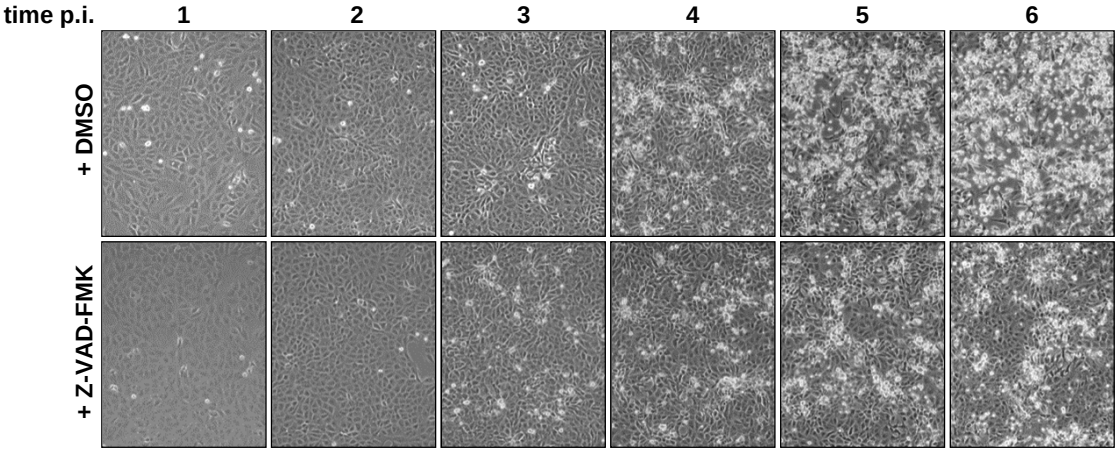
time p.i.
1
2
3
4
5
6
+ DMSO
+ Z-VAD-FMK

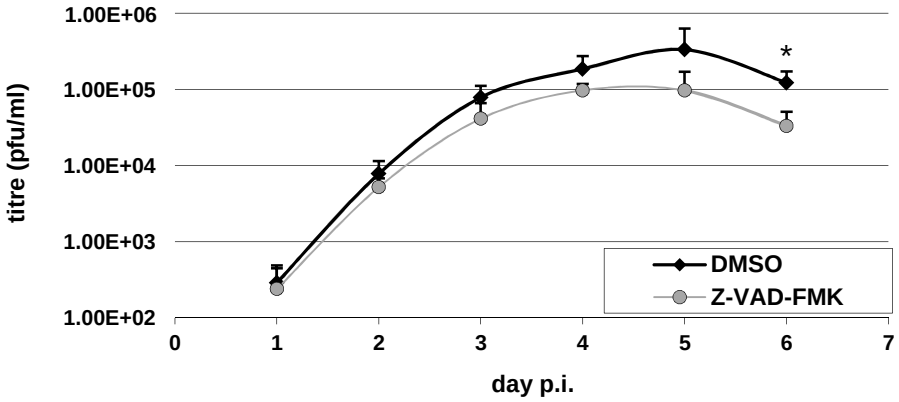
1.00E+06
1.00E+05
1.00E+04
1.00E+03
1.00E+02
titre (pfu/ml)
0
1
2
3
4
5
6
7
day p.i.
*
DMSO
Z-VAD-FMK

(b)

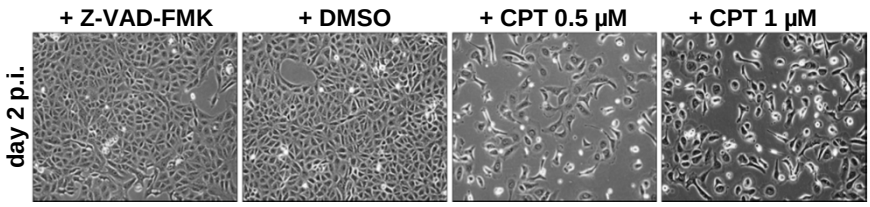
+ Z-VAD-FMK
+ DMSO
+ CPT 0.5 µM
+ CPT 1 µM
day 2 p.i.

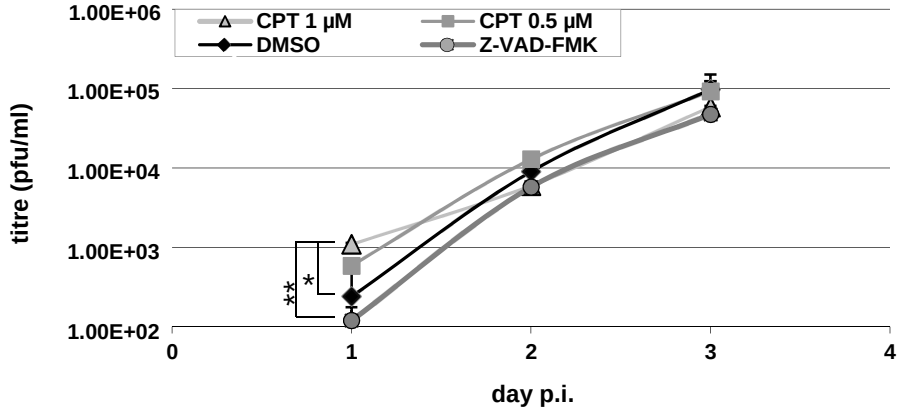
1.00E+06
1.00E+05
1.00E+04
1.00E+03
1.00E+02
titre (pfu/ml)
CPT 1 µM
CPT 0.5 µM
DMSO
Z-VAD-FMK
**
*
0
1
2
3
4
day p.i.